The Journal of Experimental Biology 202, 253–265 (1999)
Printed in Great Britain © The Company of Biologists Limited 1999
JEB1746

EXPANSION OF THE TUNICA ALBUGINEA DURING PENILE INFLATION IN THE NINE-BANDED ARMADILLO (*DASYPUS NOVEMCINCTUS*)

D. A. KELLY*

Department of Zoology, Duke University, Durham, NC 27708, USA

*Present address: Department of Biomedical Sciences, Division of Anatomy, College of Veterinary Medicine, Cornell University, Ithaca, NY 14853, USA (e-mail: dak20@cornell.edu)

Accepted 12 November 1998; published on WWW 11 January 1999

Summary

Artificial inflation of corpora cavernosa from the nine-banded armadillo (*Dasypus novemcinctus*) showed that the expansion of the tunica albuginea during erection increases both components of flexural stiffness: the second moment of area and Young's modulus of elasticity. Folded tissue and crimped collagen fibers in the tunica albuginea permit its expansion during erection. As the tunica albuginea's radii increase in size, its second moment of area also increases. The crimped collagen fibers permit the flaccid tunica albuginea to expand to strains of 25 % longitudinally and 15 % circumferentially, after which tissue stiffness increases by 3–4 orders of magnitude. Radial expansion of the corpus cavernosum is limited by collagenous trabeculae. The trabeculae maintain the non-circular cross section of the corpus cavernosum during erection. Restricting expansion appears to protect the corpus spongiosum and urethra from occlusion, but has the side effect of reducing the potential flexural stiffness of the corpus cavernosum by reducing the second moment of area of the tunica albuginea.

Key words: armadillo, *Dasypus novemcinctus*, tunica albuginea, penis, inflation, elasticity, flexural stiffness, hydrostat, collagen.

Introduction

Before a male mammal copulates, his normally inconspicuous penis changes both its size and its resistance to bending or 'flexural stiffness'. Starting as a small and highly flexible structure, the penis becomes larger and more rigid, until it is stiff enough to enter the female's vaginal opening without bending. The increase in penile size and flexural stiffness is the result of the vascular engorgement of a cylindrical structure in the mammalian penis called the corpus cavernosum (Deysach, 1939; Creed et al., 1991).

How does the anatomical design of the corpus cavernosum allow it to become temporarily rigid for intromission? If the corpus cavernosum used rigid materials in its construction, it would automatically have the high flexural stiffness it needs during copulation. Indeed, intromittent organs in many other organisms are reinforced by hard skeletons: the claspers of elasmobranchs and the gonopodia of some groups of teleost fish are modified anal fins supported by cartilage or bone (Wourms, 1981; van Tienhoven, 1983; Dodd and Dodd, 1985), insect aedeagi are supported by chitin and scleroprotein (Eberhard, 1985) and nematode spicula are supported by sclerotized cuticle (Hyman, 1951). However, the use of rigid materials means that the reproductive structures are permanently rigid. The mammalian corpus cavernosum is one example of an inflatable intromittent organ; among vertebrates, similar structures are found in caecilians (Wake, 1998), squamates (Dowling and Savage, 1960; King, 1981), turtles (Zug, 1966; King, 1981), crocodilians (King, 1981) and some birds (King, 1981).

The corpus cavernosum (Fig. 1) is made up of a central network of interconnected spaces lined with endothelial and vascular tissue surrounded by a wall of collagenous tissue called the tunica albuginea (Walton, 1956; Nickel et al., 1979; Ashdown, 1987). During erection, the interconnected spaces fill with blood and place the tunica albuginea into tension (Purohit and Beckett, 1976). This interaction between a pressurized fluid and a membrane in tension identifies the corpus cavernosum as a hydrostatic system (Wainwright et al., 1976).

Like other hydrostats (Wainwright et al., 1976, 1978; Neville, 1993), the wall of the corpus cavernosum is reinforced against aneurysms by a highly organized array of inextensible fibers. But the arrangement of the tunica albuginea's fiber array is unusual for a biological hydrostat. Instead of being arranged in left- and right-handed helices around the long axis of the structure, collagen fibers are arranged in an axial orthogonal array with fibers at 0 ° and 90 ° to the long axis of the corpus cavernosum (Hanyu, 1988; Hsu et al., 1994a,b; Kelly, 1997). A hydrostat reinforced by an axial orthogonal array has a higher flexural stiffness than similar structures reinforced by crossed-helical fiber arrays (Koehl et al., 1995; Kelly, 1997), a feature that helps prevent the corpus cavernosum from bending during copulation. But axial orthogonal arrays also

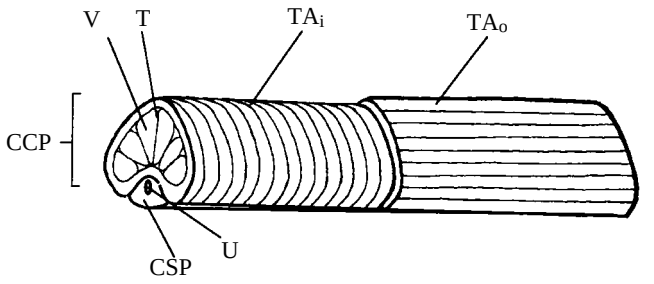

Fig. 1. Diagram of an erect, skinned *Dasypus novemcinctus* penis showing a transverse section on the left and the inner (TA$_i$) and outer (TA$_o$) layers of the tunica albuginea viewed longitudinally. CCP, corpus cavernosum; CSP, corpus spongiosum; U, urethra; V, vascular space of CCP; T, trabeculum.

resist elongation because the fibers parallel to the structure's long axis resist forces that place them in tension (Wainwright, 1988; Kelly, 1997).

How, then, does the corpus cavernosum change size during erection? Collagen fibers in the axial orthogonal array are only extended and in tension when the corpus cavernosum is erect. When flaccid, the tunica albuginea is deeply folded and the collagen fibers within it are highly crimped (Hanyu, 1988; Hsu et al., 1994a,b; Kelly, 1997). The folded tissue and crimped collagen fibers allow the tunica albuginea to expand during erection; it has been suggested that penile extensibility is due entirely to this morphology (Tejada et al., 1991; Goes et al., 1992). Expansion of the tunica albuginea may also be instrumental in increasing penile stiffness by increasing the flexural stiffness of the corpus cavernosum.

Expansion and the increase in corpus flexural stiffness during erection

If the corpus cavernosum is modeled as a beam, its flexural stiffness, *F*, is a composite variable derived from the product of two components: a material property, Young's modulus of elasticity, *E*, which is a measure of the stiffness of the material, and a geometric measure, the second moment of area, *I*, which describes the distribution of tissue around a central plane of bending:

$$F = EI\,. \tag{1}$$

Increasing the value of either or both of these components will increase the flexural stiffness of the beam.

As the tunica albuginea unfolds during erection, the change in collagen fiber orientation should increase the Young's modulus of the tissue. Folded collagenous tissue has been described in other expandable biological systems such as mammalian arterial wall (Fung, 1981, 1984; Canfield and Dobrin, 1987), the throat of the fin whale (*Balaenoptera physalus*) (Orton and Brodie, 1987) and the skin of an inflating pufferfish (*Diodon holocanthus*) (Brainerd, 1994). All these tissues contain collagen fibers arranged in crossed helices around the long axis of the structure, but they are also deeply folded and contain crimped collagen fibers. When these structures inflate, the tissue is initially compliant and expands. The stiffness of the tissue increases when collagen fibers in the tissue are straightened; the amount of extension that occurs before stiffness increases depends upon the degree of folding and fiber crimping within the tissue. Pufferfish skin, for example, reaches strains of 40–50 % before its stiffness begins to increase (Brainerd, 1994).

Little is known about the actual material properties of the tunica albuginea. Studies of human tunica albuginea (Bitsch et al., 1990; Hsu et al., 1994a) have been unable to obtain an accurate measure of the tissue stiffness or how it changes during erection. Tejada et al. (1991) and Kelly (1997) predict that the tunica albuginea will also have nonlinear material properties: the unstressed folded tissue will be compliant, and wall stiffness will increase as the tissue is stretched during erection as a result of collagen fiber recruitment.

The crimped collagen fibers and three-dimensional folding of the tissue in the flaccid tunica albuginea also permit the corpus cavernosum to expand in length and radius during erection (Tejada et al., 1991). The radial expansion of the tunica albuginea may also be related to the increase in flexural stiffness of the corpus cavernosum during erection, because an increase in the overall radius of the corpus cavernosum should increase its second moment of area.

The second moment of area, *I*, is one factor that contributes to the flexural stiffness of a structure; it describes the distribution of structural material lateral to a bending plane. It is proportional to radius raised to the fourth power in a hollow circular cylinder:

$$I = \int_{r_i}^{r_o} r^2 \mathrm{d}A \propto r_o^4 - r_i^4\,, \tag{2}$$

where r is the radius of the structure (with r_o representing the outer radius and r_i the inner radius of the structure) and A is the cross-sectional area of the material in the structure (Smith and Sidebottom, 1969). Small changes in the erect radius of the structure could therefore have a very large effect on the structure's stiffness in bending. Although increases in the second moment of area are strictly related to increases in the flexural stiffness of a rigid homogeneous beam (Smith and Sidebottom, 1969), this variable has been used to approximate changes in flexural stiffness in fiber-wound pressurized structures with an outer wrapping in tension (Spencer, 1972).

Restriction of corpus expansion during erection?

The corpus cavernosum contains another anatomical feature that could affect its expansion and its erect flexural stiffness – a network of collagenous cords called trabeculae that traverse the vascular space of the corpus cavernosum. Trabeculae (Fig. 1) originate on the inner surface of the tunica albuginea, span the vascular space and connect the dorsal and ventral sides of the corpus (Walton, 1956; Nickel et al., 1979; Ashdown, 1987). Goldstein et al. (1985) suggest that the functional role of the trabeculae is to increase the flexural stiffness of the corpus cavernosum in the same way that metallic struts can increase the

flexural stiffness of a hollow metallic structure by reinforcing its interior against bending. In fact, the trabeculae cannot stiffen the corpus cavernosum in bending because reinforcing a hollow structure with struts spanning its central space is only effective when it uses materials strong in axial compression. Collagen fibers only effectively resist tensile forces (Wainwright et al., 1976), and bending the corpus cavernosum will take the trabeculae out of tension. Instead, the trabeculae appear to be responsible for maintaining the corpus cavernosum's non-circular cross-sectional shape during erection by restricting the radial expansion of the corpus cavernosum.

A hollow, fluid-filled, cylindrical structure should tend to become more circular in cross section as its internal volume increases, because the pressure on the wall of the structure is equally distributed over the internal surface of the structure (Wainwright, 1988). But mammalian corpora cavernosa are not only non-circular in flaccid cross section (see, for example, Ashdown, 1973; Woolley and Webb, 1977; Arvy, 1978; Goldstein et al., 1985; Ribeiero and Noguiera, 1990; Woodall, 1995); comparisons of flaccid and erect human corpora (Goldstein et al., 1985) show that the non-circular cross-sectional shape is maintained in the erect corpus cavernosum.

Like the collagen fibers in the tunica albuginea, collagen fibers in human trabeculae are crimped along their long axes when the corpus cavernosum is flaccid and straighten during erection (Goldstein et al., 1985). Trabecular straightening would allow the corpus cavernosum to expand radially during erection. But the radial expansion of the corpus cavernosum could be restricted if the fully extended trabeculae are shorter than the maximum potential radius of the inflated corpus cavernosum. By restricting the maximum radius of the corpus cavernosum, the trabeculae could reduce the maximum flexural stiffness of the structure by reducing its maximum potential second moment of area.

In this study, I examine the changes in both components of flexural stiffness during erection in the corpus cavernosum. I describe the morphological changes in the corpus cavernosum during erection to determine whether its second moment of area increases during erection and whether the collagenous trabeculae limit its radial expansion. I also artificially inflate the tunica albuginea to determine the changes in its extensibility and stiffness during erection. Artificial inflation is a biaxial mechanical test that mimics the natural loading regime of the tissue (Canfield and Dobrin, 1987; Shadwick, 1992). For both parts of the study, I use the nine-banded armadillo (*Dasypus novemcinctus*) as a model. The nine-banded armadillo has the penile morphology most common among mammals, a vascular corpus cavernosum without additional stiffening mechanisms such as a penile bone or a very high concentration of collagenous tissue in the corpus (Walton, 1956; Nickel et al., 1979).

Materials and methods

Measurement of morphological changes during erection

Twenty-eight male nine-banded armadillos (*Dasypus novemcinctus* Linnaeus) were collected within 32 km of Tall Timbers Research Station near Tallahassee, Florida, USA. All these individuals were dead when collected: 26 had been killed by motor vehicles within 2 h of collection; two were donated by local hunters within 1 h of being killed.

Penile tissue distal to the ischial attachment of the corpus cavernosum was removed from each individual, skinned, and cut transversely immediately distal to the split of the penile crurae to expose the vascular space of the corpus cavernosum. Specimens ranged from 39.2 to 49.4 mm in flaccid length. Thirteen flaccid penises were fixed immediately in 10 % buffered formalin (Kier, 1992). In the remaining 15 penises, the exposed opening to the vascular space was tied shut with cotton thread; vascular tissue and trabeculae were cut with surgical scissors in five corpora before closing. These corpora were injected with 10 % buffered formalin until fluid leaked out of the tied opening to the vascular space, indicating that the corpus was at or near maximum erect volume. Erect corpora were immersed in 10 % buffered formalin. After being fixed for at least 48 h, each specimen was transferred into 70 % ethanol.

When corpora were artificially inflated, dial caliper measurements of external penile length, dorsoventral diameter and lateral diameter were taken to a precision of 0.1 mm before and immediately after inflation to document their change during erection. For each measurement, the penis was placed on a table, and the calipers were closed on either side of a pair of landmarks until they just touched the tissue. External penile length was defined as the distance between the distal opening of the urethra and the proximal split of the crura of the corpus cavernosum. External dorsoventral and lateral diameters were measured near the distal end of the penis, immediately proximal to a pair of bumps produced by the corpus spongiosum. Three repeated measurements of these variables were within 0.3 mm in all cases.

After fixation, a 1 cm thick transverse section from the middle of the penile shaft was cut from each corpus. Internal dorsoventral diameter, lateral diameter and wall thickness were measured from each corpus using dial calipers to a precision of 0.1 mm (three repeated measurements were within 0.2 mm). Internal diameters were measured at the lateral and dorsoventral midlines of the corpus cavernosum. The thickness of the tunica albuginea was measured at three locations around the circumference of the corpus cavernosum, and the values were averaged.

Each 1 cm thick transverse section was photographed on a 1 cm grid with a 35 mm SLR camera oriented parallel to the section at a height of 15 cm. Photographs of corpora cross sections were scanned into computer files using a digital scanner (HP ScanJet IIcx supported by DeskScan II 2.0) and examined using Image 1.33f (National Institutes of Health) to determine the angle of the corpus cavernosum over the urethra and the exposed cross-sectional area of the corpus cavernosum. The urethral angle was measured by digitizing the two ventralmost points of the tunica albuginea and the point on the tunica albuginea immediately dorsal to the urethra (Fig. 2A) and calculating the angle between these points. Three repeated measurements were within 2 ° of one another. The cross-sectional area of each corpus was determined by digitizing points around the outer edge of the tunica albuginea. Measurements repeated three times were within 0.05 cm^2 of one another.

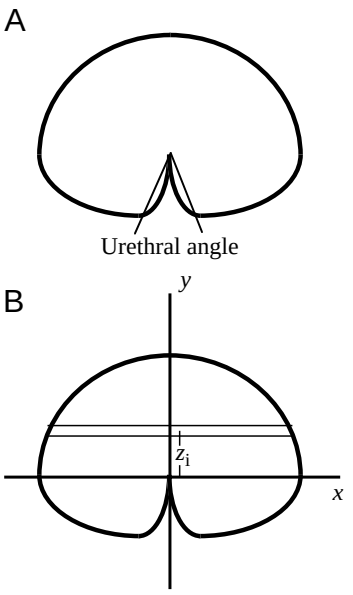

Fig. 2. Schematic diagram of the *Dasypus novemcinctus* corpus cavernosum in cross section. (A) Definition of the urethral angle. The angle between the two ventralmost points on the tunica albuginea and the point on the tunica albuginea immediately dorsal to the urethra was measured. (B) Location of the *x*- and *y*-axes used in calculations of second moment of area. The *x*-axis is the neutral axis for bending in the dorsoventral direction; the *y*-axis is the neutral axis for bending laterally. The point at which the two axes cross is the centroid of the cross section. One strip of area used in the calculation of the second moment of area of the tunica albuginea over the dorsoventral axis of the corpus cavernosum, I_x, is shown to demonstrate the method; z_i is the distance of the strip's center from the neutral axis.

To determine the second moments of area of the tunica albuginea, four outlines of each corpus cross section were traced onto thin cardboard from the photographs of the corpora. Two of these outlines were areas bounded by the outer edge of the tunica albuginea (A_o), two were areas bounded by the inner edge of the tunica albuginea (A_i). The outlines were cut out, and the centroid was located on each by hanging the outline from a pin on its periphery and drawing a vertical line directly under the pin to bisect the shape. This procedure was repeated three times at randomly chosen locations around the periphery of the shape. Because the centroid is equivalent to the outline's center of gravity, the point where the three lines intersect is a good approximation of its location (Denny, 1988). Centroids were in equivalent locations for both inner and outer boundaries.

Once the centroid of the shape had been located, a line was drawn through it to represent a neutral surface of the corpus cavernosum in bending. Although there are theoretically an infinite number of neutral surfaces through the corpus cavernosum, two were selected for analysis: the neutral axis through the dorsoventral midline of the corpus cavernosum, and the neutral axis through its sagittal midline. For the remainder of this discussion, these planes will be referred to, respectively, as the *x*-axis and the *y*-axis (Fig. 2B).

Each cut-out was cut into approximately ten strips with centers at measured distances (z) from a neutral surface. The area of each strip was determined by weighing it against a cardboard standard of known area. The scale weighed strips to a precision of 0.001 g, and ten repeated measurements of a 200 mg standard weight were within 0.003 g of one another. To test the repeatability of the cutting technique, ten 4 mm strips of the same material used to make the cut-outs were cut and weighed; the weights of these strips were within 0.005 g of one another. The weight of an uncut outline and the summed weights of its component strips differed by less than 5 %.

The second moment of area (I) was calculated for each outline using the formula:

$$I = \sum_{i=1} a_i(z_i)^2 , \quad (3)$$

where a_i was the area of a strip and z_i was the distance of its center from the neutral axis (Denny, 1988). The second moment of area of the tunica albuginea (I_{TA}) was calculated by subtracting the second moment of area of the inner cross section (I_{Ai}) from that of the outer cross-section (I_{Ao}). Values of I_{TA} were averaged for the thirteen flaccid corpora, ten unaltered erect corpora and five erect corpora with cut trabeculae.

A section of each corpus was cut sagittally along its midline and examined using brightfield microscopy to determine the angles of the trabeculae with respect to the long axis of the corpus cavernosum. Angles were measured against ocular cross-hairs using a stage goniometer to a precision of 0.1 ° (three repeated measurements were within 0.3 °). Twenty-one angles from flaccid corpora and forty-one angles from erect corpora were averaged and compared.

The results are expressed as means ± S.E.M., unless stated otherwise, and were compared using Student's *t*-tests with SYSTAT 5.2 (SYSTAT, Inc.).

Materials testing

Nine male nine-banded armadillos (*Dasypus novemcinctus*) were obtained for experimentation: five were collected within 32 km of Tall Timbers Research Station near Tallahassee, Florida, USA, within 2 h of being killed by cars; four were obtained from a supplier (Ray Singleton & Company) and killed with an overdose of sodium pentabarbitol administered intracardially (Duke University IACUC protocol A614-95-9R2). Carcasses were either incinerated or used for other studies after the tissue of interest had been removed.

Penile tissue distal to the ischial attachment of the corpus cavernosum was removed from each individual. Penises ranged from 36.0 to 49.2 mm in flaccid length. The skin and the proximal part of the dorsal retractor muscle were removed from the penis, but the corpus spongiosum was left intact. Pieces of pencil lead 5 mm long and 0.5 mm thick were attached to the external surface of the tunica albuginea using cyanoacrylate glue as markers for longitudinal tissue displacement. Markers were placed approximately 20 mm apart and at least 1 cm away from the proximal and distal ends of the corpus cavernosum to avoid end effects.

The corpus cavernosum was cut transversely immediately distal to the split of the penial crurae to expose its vascular space, and the trabeculae were cut with surgical scissors. Removing the trabeculae meant that artificial inflation would allow measurement of the material properties of the tunica albuginea alone. When the trabeculae had been removed, the proximal opening of the vascular space was tied shut with cotton thread. The corpus was injected with mammalian physiological saline (Kiernan, 1990) at the proximal opening of the vascular space to ensure that no leaks were produced by tissue preparation. The cotton thread was removed, and all the saline was squeezed out of the vascular space before the start of the experiment. Tissue was tested within 3 h of collection.

After tying the proximal end of the corpus cavernosum shut with cotton thread, a 26 gauge syringe needle was placed into the empty vascular space, and the corpus was attached to the inflation apparatus. The inflation apparatus consisted of a 10 ml syringe clamped into a metal bracket. Turning a screw at one end of the bracket pushed on a Plexiglas bar attached to the syringe plunger. Each full turn of the screw released 0.13±0.01 ml (mean ± S.E.M.) of fluid; the screw was calibrated by collecting the fluid released by one full turn in a 1 ml tuberculin syringe marked in 0.01 ml increments (ten repeated measurements were within 0.01 ml).

The corpus was inflated with physiological saline until adding fluid forced saline to leak from the proximal opening of the corpus cavernosum. This indicated that the structure was at maximum volume. Before and after each volumetric addition, the corpus was photographed from above and laterally to record dimensional changes. Changes in corpus cavernosum length, dorsoventral diameter and lateral diameter during inflation were measured from 4 inch×5 inch (10.2 cm×12.7 cm) prints (magnification approximately 2×) of these photographs using dial calipers to a precision of 0.1 mm (measurements repeated three times were within 0.2 mm). A 1 cm scale bar was included on the experimental apparatus to ensure that all photographs were enlarged to the same magnification. In each photograph, corpus length was measured from the outside edges of the pieces of pencil lead, and corpus diameters were measured from the extreme dorsoventral or lateral edges of the corpus.

Changes in intracavernosal pressure during inflation were measured to a precision of 1 kPa using a miniature pressure transducer (Precision Measurements, model 060S, 0–690 kPa) inserted into the exposed proximal end of the vascular space. The pressure transducer made up one arm of an ordinary direct-current Wheatstone bridge; the voltage across the bridge was amplified by an auto-zeroing instrumentation amplifier (Intersil ICL-7605-CJN used in the manufacturer's recommended circuit). Voltage levels were displayed on an oscilloscope (BK Precision Instruments, model 2120A, 20 MHz).

The miniature pressure transducer was calibrated against the gauge of a Scholander pressure bomb (PMS Instrument Co.) with a linear extrapolation to lower pressures. The calibration of the gauge on the pressure bomb was subsequently checked against a U-tube mercury manometer; the pressure bomb gauge gave measurements on average 7 % below those determined using the manometer. Pressure changes were successfully recorded for only three corpora: since the differences among these data sets were small (±1 kPa), the traces were averaged and the average pressure was used in all stress calculations.

Changes in tissue dimensions and intracavernosal pressure were used to calculate true stress and strain in the tunica albuginea after each volumetric addition. Because the cross-sectional area of the tunica albuginea changes during erection, stress was calculated as force divided by the cross-sectional area of the tunica albuginea at each volumetric addition. Since trabeculae were removed from the vascular space before testing, I assumed that the tunica albuginea could expand without restriction and that the corpus cavernosum could therefore be modeled as a cylinder with a circular cross section. Because the mean wall thickness of erect corpora without trabeculae (0.8 mm, from Table 1) was more than 10 % of the mean radius of the corpora, the corpus cavernosum was modeled as a thick-walled cylinder. The formulae for instantaneous stress σ in the tunica albuginea were therefore:

$$\sigma_L = Pr_c/2t\,, \tag{4}$$

$$\sigma_C = P[r_i^2/(r_c^2 - r_i^2)][1 + (r_c^2/r_i^2)]\,, \tag{5}$$

where σ_L is longitudinal stress, σ_C is circumferential stress, P is the instantaneous mean intracavernosal pressure, t is the mean thickness of the outer layer of longitudinal fibers in erect corpora (0.24 mm, from Kelly, 1997), r_c is the instantaneous inner radius of the outer layer of the tunica albuginea, and r_i is the instantaneous inner radius of the inner layer of the tunica albuginea (Timoshenko, 1957; Wainwright et al., 1976). Because it was impossible to measure changes in tunica albuginea thickness during the inflation experiment, I assumed that the thicknesses of the collagen fiber layers of the tunica albuginea remained constant, although the tissue layers actually become thinner as the tunica albuginea expands during inflation (Kelly, 1997). Using the mean thickness of erect tunica albuginea in these calculations means that values for instantaneous stress will be overestimated at low levels of inflation, but will become more accurate at higher levels.

True strain ε in the tunica albuginea was calculated directly from the dimensional changes of the corpus cavernosum because of the large extensions of the tissue during erection:

$$\varepsilon = \ln[l_i/l_o]\,, \tag{6}$$

where l_i is the instantaneous length of the tissue in one direction of loading and l_o is the original length of the tissue in that direction (Wainwright et al., 1976). Strains for each axis were averaged and compared with changes in internal volume and mean intracavernosal pressure.

Where appropriate, longitudinal stress was plotted against longitudinal strain; circumferential stresses were plotted against circumferential strains. Tissue stiffness E in each direction was calculated as the slope of a stress–strain curve, where:

$$E = d\sigma/d\varepsilon\,. \tag{7}$$

Although it is ordinarily desirable to calculate Young's

modulus while correcting for the interaction between longitudinal and circumferential strains with the appropriate Poisson's ratios (Vincent, 1990), this correction is unnecessary in the case of the corpus cavernosum because it contains two independent longitudinal and circumferential fiber systems that do not interact significantly with one another during inflation.

Data were averaged and checked for statistical significance using Kolmogorov–Smirnov tests (SYSTAT 5.2, SYSTAT, Inc.). The results are presented graphically, and major features are reported as means with the standard error of the mean (S.E.M.) shown in parentheses.

Results

Gross morphological changes upon erection

During erection, the penis increases by an average of 29.0 % in length, by 16 % across its external dorsoventral diameter and by 17 % across its external lateral diameter. Measurements from flaccid and erect cross sections show that the internal dorsoventral diameter of the corpus cavernosum increases by an average of 50 % during erection, while internal lateral diameters increase by 25 %. Tunica albuginea thickness decreases by an average of 39 % during erection (Table 1).

The exposed cross-sectional area of the corpus increases by an average of 78 % during erection, from a value of $4.5\times10^{-5}\pm0.3\times10^{-5}\,m^2$ to a value of $8.0\times10^{-5}\pm0.6\times10^{-5}\,m^2$. Cross-sectional shapes remain non-circular after inflation (see Fig. 3), and the urethral angle decreases from 122±2.9 ° in flaccid corpora to 98±2.4 ° in erect corpora (Table 1).

The trabeculae are oblique to the long axis of the corpus cavernosum, slanted proximally at an angle of 84.0±1.2 ° in flaccid corpora and of 80.0±0.8 ° in erect corpora (Table 2). Collagen fibers in the armadillo trabeculae are crimped along their long axis when flaccid and straighten during erection, causing a 53 % increase in trabecular length. The longitudinal distance between the dorsal and ventral attachments of the trabeculae also increases by 167 % during erection (Table 2).

Student's *t*-tests (Table 3) show that all morphological differences between flaccid and erect corpora are significant to at least the 5 % level. Most are significant at the 0.1 % level.

Changes in second moment of area

The mean second moment of area of the tunica albuginea over the dorsoventral axis of the corpus cavernosum (I_x) increases by 150 % during erection, from $1.0\times10^{-9}\pm0.1\times10^{-9}\,m^4$ in flaccid corpora to $2.5\times10^{-9}\pm0.6\times10^{-9}\,m^4$ in erect corpora (N=13 flaccid and N=10 erect; t=–2.8; P=0.01). Similarly, the mean second moment of area of the tunica albuginea over the lateral axis of the corpus cavernosum (I_y) increases by 110 % during erection, from $3.0\times10^{-9}\pm0.6\times10^{-9}\,m^4$ in flaccid corpora to $6.3\times10^{-9}\pm1.0\times10^{-9}\,m^4$ in

Table 1. *Averaged measurements of* Dasypus novemcinctus *penis before and after inflation*

		Erect	
	Flaccid	Unaltered	Altered
External penile dimensions	N=10	N=10	N=5
Length (mm)	43.5±0.8	56.1±1.5	56.6±1.5
Dorsoventral diameter (mm)	9.2±0.4	10.7±0.4	11.2±0.4
Lateral diameter (mm)	8.3±0.2	9.7±0.3	9.5±0.2
Corpus cavernosum dimensions	N=13	N=10	N=5
Dorsoventral diameter (mm)	3.0±0.2	4.5±0.2	7.8±0.6
Lateral diameter (mm)	9.6±0.3	12.0±0.3	13.3±0.3
Wall thickness (mm)	1.3±0.1	0.8±0.0	0.8±0.1
Cross-sectional area $\times10^{-5}$ (m^2)	4.5±0.3	8.0±0.6	12.2±0.6
Urethral angle (degrees)	122±2.9	98±2.4	140±13.4

Unaltered specimens had intact trabeculae; in altered specimens, the trabeculae had been cut.

Specimens ranged from 39.2 to 49.4 mm in flaccid length.

The table lists changes in both external penile dimensions and corpus cavernosum dimensions.

Flaccid and unaltered erect external penile measurements are from the distal portion of the same specimens before and after inflation, but measurements of the flaccid and erect corpus cavernosum are from more proximal regions of different treatments.

The number of specimens in each sample is given at the top of each column of measurements.

Values are means ± S.E.M.

Table 2. *Change in trabecular angle and related corpus cavernosum dimensions upon erection*

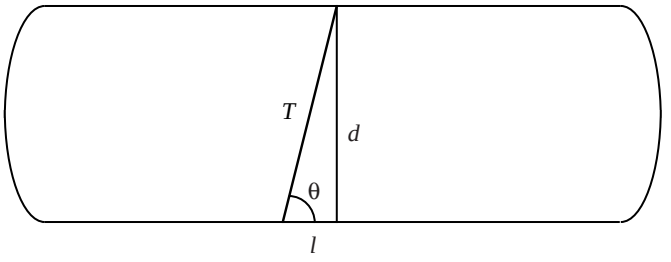

	Flaccid	Erect	% Change
Number of measurements	21	41	–
Trabecular angle, θ (degrees)	84.0±1.2	80.0±0.8	4.8
Dorsoventral diameter, d (mm)	3.0±0.2	4.5±0.2	50
Trabecular length, T (mm)	3.0	4.6	53
Longitudinal distance between dorsal and ventral attachments, l (mm)	0.3	0.8	167

The outline illustrates the position of the trabeculum in relation to the long axis of the penis.

Mean trabecular angle (θ) and mean internal dorsoventral diameter (d) were measured from *Dasypus novemcinctus* corpora; trabecular length (T) and the longitudinal distance between the dorsal and ventral attachments of a trabeculum (l) were estimated using trigonometry.

Values are means ± S.E.M.

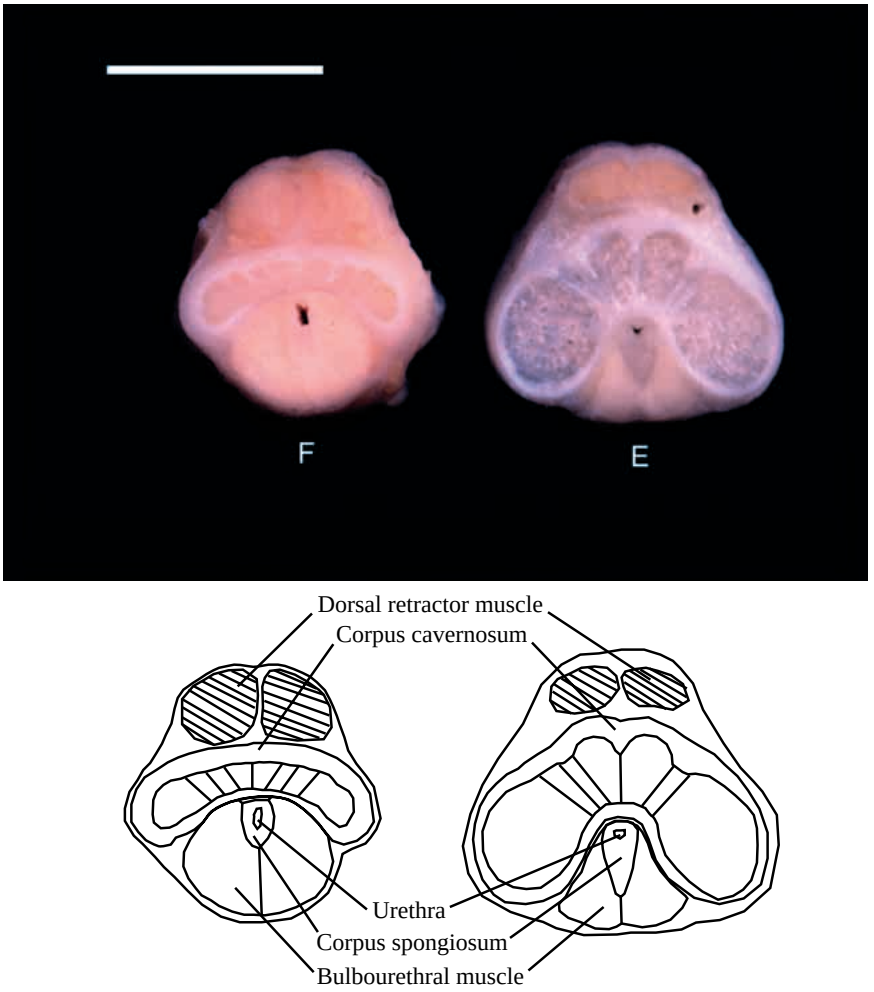

Fig. 3. Transverse sections of *Dasypus novemcinctus* corpora cavernosa showing changes in internal morphology after artificial erection. F, flaccid; E, erect. Scale bar, 1 cm. The accompanying schematic diagram identifies major anatomical features. Both sections were taken from the proximal end of the free part of the penis; in flaccid penises, there is a larger amount of variation in the cross-sectional area of the penis retractor muscle owing to differing amounts of contraction at fixation.

erect corpora (N=13 flaccid and N=10 erect; t=–3.0; P=0.007) (Table 4).

Because the corpus cavernosum has a lower intracavernosal pressure when it is flaccid, its tunica albuginea is probably not in tension. Therefore, the values calculated for the flaccid samples approximate the second moments of area found when

Table 3. *Results of Student's* t*-tests comparing morphological changes in penile tissue*

	Flaccid *versus* erect			Erect unaltered *versus* altered		
	N	*t*-statistic	*P*	*N*	*t*-statistic	*P*
External penile dimensions						
Length	10	–7.42	<0.0001	10; 5	–0.25	0.808
Dorsoventral diameter	10	–2.73	0.014	10; 5	–0.72	0.483
Lateral diameter	10	–3.94	0.001	10; 5	0.66	0.523
Corpus cavernosum dimensions						
Dorsoventral diameter	13; 10	–6.21	<0.0001	10; 5	–7.20	<0.0001
Lateral diameter	13; 10	–5.83	<0.0001	10; 5	–2.68	0.019
Wall thickness	13; 10	5.60	<0.0001	10; 5	–0.13	0.895
Cross-sectional area	13; 10	–5.47	<0.0001	10; 5	–4.31	0.001
Urethral angle	13; 10	6.25	<0.0001	10; 5	–4.30	0.001
Trabecular angle	21; 41	2.87	<0.0001	–	–	–

N, number of individuals in the samples compared.

When samples do not contain the same number of individuals, values of *N* are listed in the same order as the compared samples. For example, *N* for *x versus y* would be written n_x;n_y.

In altered tissue, the trabeculae had been cut.

Table 4. *Mean values of the second moment of area of the tunica albuginea in flaccid and erect* Dasypus novemcinctus *corpora cavernosa*

		Erect	
	Flaccid	Unaltered	Altered
N	13	10	5
$I_x \times 10^{-9}$ (m^4)	1.0±0.1	2.5±0.6	5.8±1.2
$I_y \times 10^{-9}$ (m^4)	3.0±0.6	6.3±1.0	7.6±1.5

I_x, I_y, second moment of area over the *x*- and *y*-axes (see Fig. 2). Values are means ± S.E.M.

the corpus cavernosum is first pressurized at the start of tumescence.

Removal of trabeculae

Although trabeculae in erect corpora originate over approximately 70 % of the dorsolateral surface of the tunica albuginea, they reattach to only approximately 20 % of the ventromedial surface of the tunica albuginea (Figs 3, 4). Thus, trabeculae viewed in the cross section of the corpus cavernosum are arranged in a fan that radiates outwards from the surface of the tunica above the corpus spongiosum and the urethra.

Erect corpora with cut trabeculae have a more circular cross-sectional shape than unaltered erect corpora (Fig. 4), caused mainly by a 73 % increase in dorsoventral expansion during erection (Table 1). This change, along with a smaller (10.8 %) increase in lateral expansion, leads to a 53 % increase in cross-sectional area in erect corpora without trabeculae to $12.2\times10^{-5}\pm0.6\times10^{-5}\,m^2$. Fig. 4 shows that the increased dorsoventral expansion of the corpus cavernosum seems to occlude the urethra, because the urethral angle increases by 43 % to a value of 140±13.4 °. Student's *t*-tests show that these changes in internal diameters, cross-sectional area and urethral angle are statistically significant (Table 3).

The second moment of area of the erect tunica albuginea is larger in corpora with cut trabeculae than in normal corpora (Table 4): I_x increases by 132 % over corpora with intact trabeculae (N=10 unaltered and N=5 altered; t=–2.8; P=0.014), but I_y does not increase significantly (N=10 unaltered and N=5 altered; t=–0.7; P=0.49).

Mechanical effects of increasing internal volume

As fluid is added to the vascular space of the altered corpus

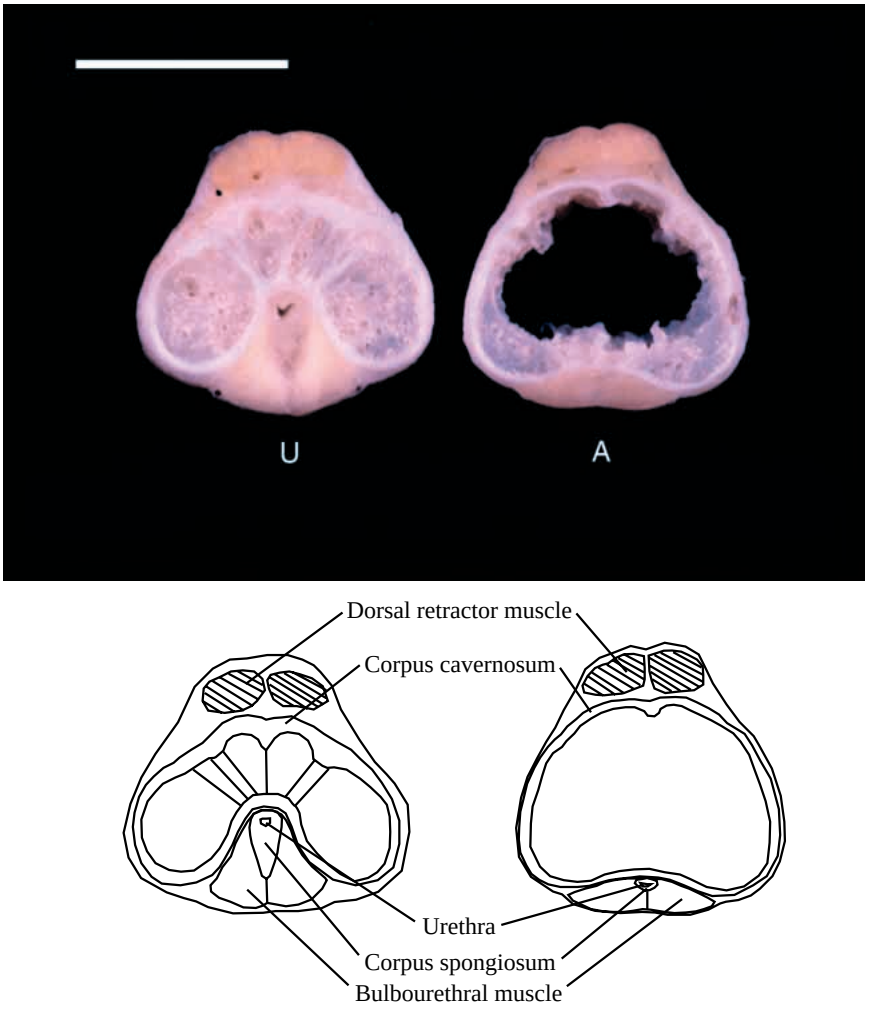

Fig. 4. Transverse sections of erect *Dasypus novemcinctus* corpora cavernosa illustrating the effects of trabeculae removal upon corpora morphology. U, unaltered, trabeculae present; A, trabeculae removed. Both corpora shown were fixed while erect. Scale bar, 1 cm. The accompanying schematic diagram identifies the major anatomical features.

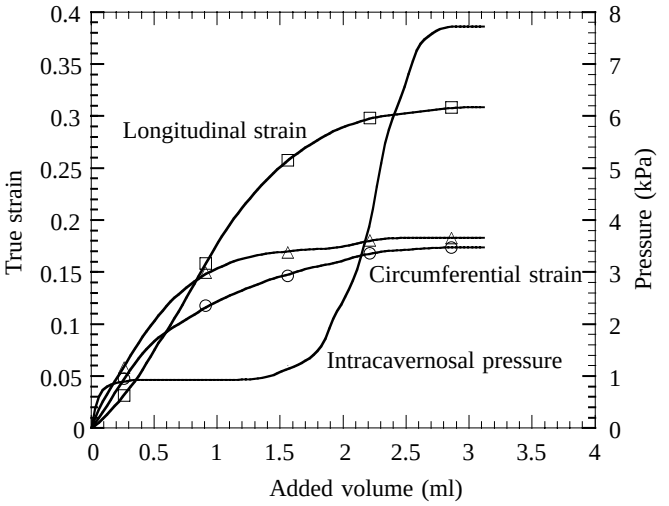

Fig. 5. Change in mean biaxial tissue strain over three axes of the altered (trabeculae removed) corpus cavernosum and mean intracavernosal pressure during artificial inflation of the tunica albuginea. Tissue strain increases over each axis as internal volume increases, but reaches a maximum value as collagen fibers in the tunica albuginea near full extension. The point at which all strain values reach their maxima represents the maximum volume of the corpus cavernosum; after this point, fluid added to the vascular space displaces an equivalent amount of fluid. Intracavernosal pressure remains constant as the tunica albuginea expands; pressure increases when the tissue reaches maximum extension. Changes in tissue strain are denoted by open symbols; squares represent strain along the long axis of the corpus cavernosum (S.E.M. ± 0.04), circles represent circumferential strain viewed laterally (S.E.M. ± 0.02) and triangles represent circumferential strain viewed dorsally (S.E.M. ± 0.03).

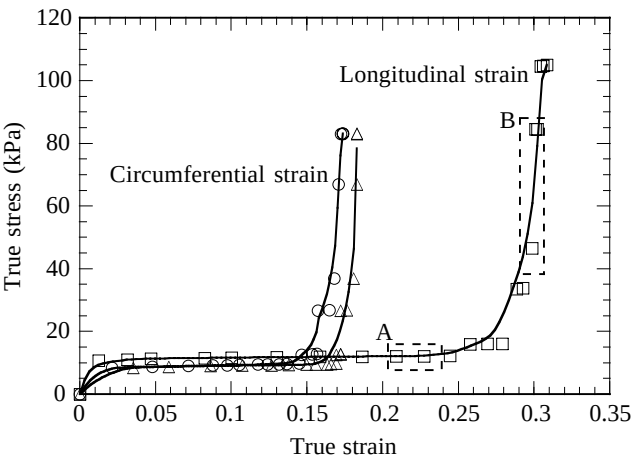

Fig. 6. Mean smooth stress–strain curves illustrating the extension of the tunica albuginea along three axes during artificial inflation. Tunica albuginea stiffness, represented by the instantaneous slope of each line in the graph, increases by 3–4 orders of magnitude once the tissue strain is 0.25 longitudinally and 0.15 circumferentially. Symbols denote the direction of tissue strain: squares represent longitudinal strain, circles represent circumferential strain viewed laterally and triangles represent circumferential strain viewed dorsally. Dotted boxes labeled A and B refer to Fig. 7A,B.

cavernosum, wall strain along each axis initially increases, but levels off at a maximum strain of 0.31±0.04 along the length of the corpus cavernosum, of 0.17±0.02 over its circumference viewed laterally (calculated from changes in the dorsoventral diameter) and of 0.18±0.03 over its circumference viewed dorsally (calculated from changes in the lateral diameter) (Fig. 5). While the wall strain along the length of the corpus cavernosum is approximately twice the wall strain along either circumferential axis (N=9, Kolmogorov–Smirnov=0.68, P=0.008), wall strains along the two circumferential axes are not significantly different from each other (N=9, Kolmogorov–Smirnov=0.36, P=0.102).

Mean intracavernosal pressure (N=3 measurements) increases slightly from ambient at the start of inflation to 1±1 kPa, then stays constant as wall strain increases (Fig. 5). Internal pressure begins to rise when strain along the circumferential axes plateaus and reaches its highest level of 8±1 kPa as the corpus cavernosum reaches maximum volume.

Wall stiffness during inflation

When inflation begins, tunica albuginea stiffness is relatively low, and it takes very little force to extend the tissue (Fig. 6). But when strains reach 25% longitudinally and 15% circumferentially, a great deal more stress is required to extend the tissue by an additional 5% longitudinally and 2% circumferentially, producing a J-shaped asymptotic curve. Wall stiffness, represented by the slope of the curve, increases by 3–4 orders of magnitude at this point; from approximately 3 kPa to 17×10^3 kPa along the longitudinal axis (Fig. 7) and from approximately 10 kPa to 10×10^3 kPa along either circumferential axis.

Discussion

Changes in tissue stiffness and second moment of area during erection

These results show that both the second moment of area and Young's modulus of the tunica albuginea increase during erection. As blood enters the vascular space of the corpus cavernosum during erection, the structure's diameters and overall cross-sectional area increase. This expansion is correlated with an increase in the second moment of area of the tunica albuginea during erection. In *Dasypus novemcinctus* corpora, the second moments of area of the tunica albuginea in unaltered erect samples were significantly larger than those of unaltered flaccid samples (t=–2.8; P=0.01). Because second moment of area is one of the components of flexural stiffness, these data suggest that the change in corpus cavernosum radius during wall expansion contributes to the increase in its overall stiffness during erection.

Because strain is a measure of tissue extension, the shape of the curves in Figs 5 and 6 reflect how increasing intracavernosal volume changes the dimensions and stiffness of the tunica albuginea. During inflation, extension is permitted

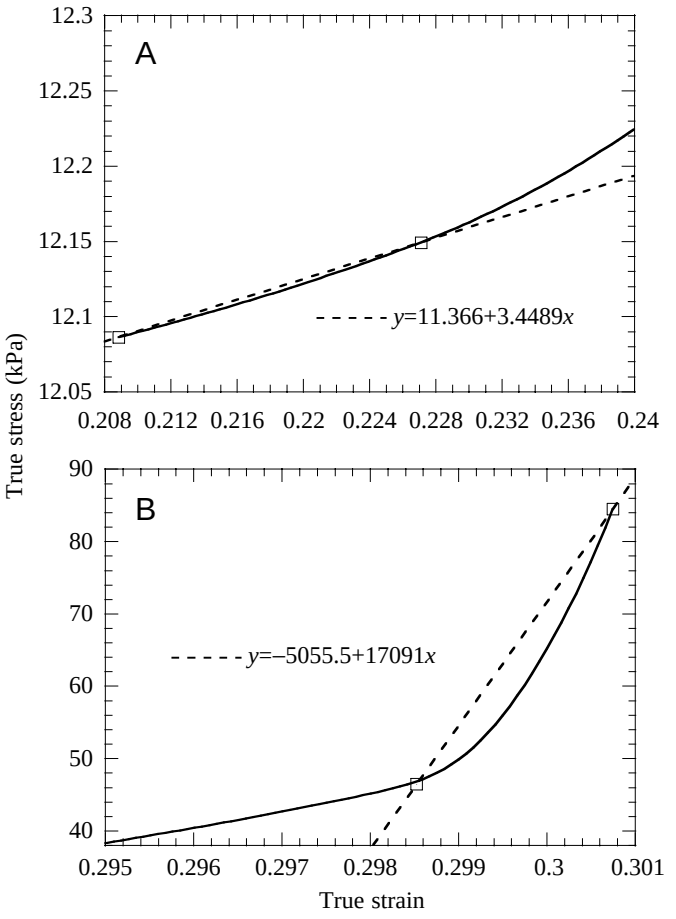

Fig. 7. Examples of regressions used to determine tunica albuginea stiffness. (A) Section of the longitudinal stress–strain curve in Fig. 6, taken from the boxed region marked A. The broken line represents a regression taken from two points (denoted by squares) in the 'shallow' part of the curve. The slope of the line at this point is approximately 3 kPa. (B) Section of the longitudinal stress–strain curve in Fig. 6, taken from the boxed region marked B. The dotted line represents a regression taken from two points (denoted by squares) in the 'steep' part of the curve. The slope of the line at this point is approximately 17×10^3 kPa.

by the straightening of crimped collagen fibers and the three-dimensional unfolding of the tissue (Tejada et al., 1991; Kelly, 1997). As the tissue unfolds, collagen fibers approach full extension and resist the tensile forces produced by further increases in internal volume. The extended collagen fibers prevent the tunica albuginea from extending by more than 30 % of its original length longitudinally and by more than 17–18 % of its original length circumferentially. The point at which all strain values reach their maxima represents the maximum volume of the corpus cavernosum; at this point, fluid added to the vascular space displaces an equal amount of fluid and causes no further increase in intracavernosal pressure.

If tunica albuginea expansion is restricted when the trabeculae are removed from the vascular space, we would expect to see differences in the circumferential tissue strains viewed in different directions. This study did not detect any statistically significant difference in circumferential strain viewed laterally and viewed dorsally, implying that the assumption of unrestricted expansion to a circular cross section in the materials tests was justified.

The tunica albuginea's material properties are nonlinear: the flaccid tunica albuginea has a relatively low stiffness and is initially compliant to inflation. Its stiffness increases asymptotically by 3–4 orders of magnitude during erection as collagen fibers in its axial orthogonal array are straightened (Fig. 6). The largest values of stiffness measured in the tunica albuginea are still considerably smaller than the tensile modulus of tendon (2×10^9 N m^{-2}, from Wainwright et al., 1976), implying that the collagen fibers in the tissue were not fully straightened during inflation; in fact, slightly crimped collagen fibers are visible in erect *D. novemcinctus* tunica albuginea (Kelly, 1997). The extended period of tissue compliance in the tunica albuginea is very similar to the material properties of other inflating collagenous tissues (Orton and Brodie, 1987; Brainerd, 1994). The large change in the tissue's modulus of elasticity should contribute to the increase in the overall flexural stiffness of the corpus cavernosum during erection.

Effect of trabeculae on cross-sectional shape and flexural stiffness

The corpus cavernosum maintains its non-circular cross-sectional shape during erection because its internal dorsal and ventral surfaces are connected by trabeculae that restrict the dorsoventral and lateral expansion of the tunica albuginea during erection. Corpora that have had their trabeculae removed have larger diameters and are more circular in erect cross section than unaltered corpora (Fig. 4).

A non-circular cross section could also be produced in the erect corpus cavernosum if the skin surrounding the penis acted as a tensile membrane during erection. In this case, the non-circular cross section would be the result of the pressure exerted on the corpus cavernosum by large structures within the penile skin such as the dorsal retractor muscle and the corpus spongiosum. However, the unaltered erect specimens used in this study retained their non-circular cross section although the skin was partially removed during preparation. In addition, penile skin remains relatively loose during erection and can easily be moved over the shaft of the erect corpus cavernosum, implying that it is not put in tension by erection (Walton, 1956).

These data suggest that the presence of trabeculae in the vascular space of the corpus cavernosum has a direct effect on the flexural stiffness of the corpus during erection. By maintaining the non-circular cross-sectional shape of the corpus cavernosum, trabeculae reduce the potential second moment of area of the tunica albuginea (Table 4). Restricting tunica albuginea expansion in the section of tissue immediately dorsal to the urethra may also locally reduce the stiffness of the tissue by not allowing the circumferentially oriented collagen fibers in that region to uncrimp fully. Restricting the potential maximum values of both the modulus of elasticity

and the second moment of area of the tunica albuginea during erection would have the ultimate effect of reducing the maximum flexural stiffness of the corpus cavernosum when erect.

Interestingly, there is no statistically significant difference in erect length between unaltered corpora and corpora that have had their trabeculae removed (t=–0.25; P=0.81), implying that the presence of trabeculae does not affect the extension of the longitudinally oriented collagen fibers in the axial orthogonal array. Increases in unaltered corpus cavernosum length during erection appear to reorient the angle of the trabeculae relative to its long axis, as the longitudinal distance between the dorsal and ventral attachments of the trabeculae increases during erection (Table 2).

If increased stiffness is required for intromission, why do mammals limit the effective stiffness of the corpus cavernosum during erection by restricting its expansion? The difference in the urethral angle of unaltered erect corpora and erect corpora with cut trabeculae suggests that the trabeculae may be preventing compression of the corpus spongiosum during erection (Table 1; Fig. 4).

A second body of erectile tissue in the penis, the corpus spongiosum (Fig. 1), lies ventral to the corpus cavernosum and surrounds the urethra. The corpus spongiosum is pressurized during erection, although it is not responsible for penile rigidity (Deysach, 1939; Vardi and Siroky, 1990). Pressure transducer measurements in dogs have shown that internal pressures in the corpus spongiosum are approximately 13 times lower than in the corpus cavernosum: during intromission, the corpus spongiosum has a mean peak internal pressure of $7.7\times10^4\pm0.8\times10^4$ Pa, as opposed to a mean peak internal pressure of $99\times10^4\pm1.2\times10^4$ Pa in the corpus cavernosum (Purohit and Beckett, 1976).

Morphological measurements of *D. novemcinctus* corpora show that corpora with cut trabeculae have a larger urethral angle than flaccid corpora. These data indicate that, when trabeculae are not present to restrict the expansion of the corpus cavernosum, the area above the urethra is flattened during erection. Unrestricted expansion of the high-pressure corpus cavernosum during erection could therefore flatten the lower-pressure corpus spongiosum, possibly preventing the effective transport of semen during ejaculation by occluding the urethra. It has been proposed that semen is propelled down the length of the penis during ejaculation by a series of pressure waves produced in the corpus spongiosum by contractions of the ischiocavernosus and bulbospongious muscles (Watson, 1964). Compression of the corpus spongiosum by the corpus cavernosum could interfere with the propagation of these waves.

When trabeculae are present in *D. novemcinctus*, the urethral angle of unaltered erect corpora is smaller than the urethral angle of flaccid corpora, so the corpus cavernosum is held away from the corpus spongiosum and the urethra during erection. By exerting laterally directed forces on the corpus spongiosum, the erect corpus cavernosum may help open the urethra to permit the passage of semen during ejaculation.

Mechanical design of the corpus cavernosum

Hemodynamic studies of the mammalian corpus cavernosum have shown that intracavernous blood pressure in flaccid corpora is lower than mean arterial blood pressure but rises to arterial levels during tumescence and erection (Wagner, 1981; Hanyu et al., 1987) and to levels much higher than mean arterial blood pressure during intromission and ejaculation (Purohit and Beckett, 1976; Hanyu et al., 1987; Andersson and Wagner, 1995). Hanyu et al. (1987) described the dog's penile erectile mechanism as follows. (1) When the penis is flaccid, the contraction of smooth muscle in the corpus cavernosum's vasculature keeps intracavernosal pressure low by restricting blood flow into the corpus. (2) During tumescence, these smooth muscles relax and permit both the inflow of blood and the expansion of the tunica albuginea. (3) As the tunica albuginea expands, it compresses the veins leaving the vascular space, reducing venous outflow and allowing the penis to remain erect. In this model, mammalian arterial blood pressure passively inflates the corpus cavernosum to full erection without the use of a pumping mechanism. A small change in intracavernosal pressure in the flaccid corpus cavernosum can thus cause a large change in intracavernosal volume and inflate the tunica albuginea.

The results of the present study agree well with this model. The folded tissue and crimped collagen fibers in the flaccid *D. novemcinctus* tunica albuginea permit tissue expansion, making the tissue initially compliant to internal volume changes. As intracavernosal volume increases, the low stiffness of the tissue means that there is little change in intracavernosal pressure. However, once the collagen fibers are straightened, their high tensile stiffness increases the stiffness of the tunica albuginea and stops further expansion of the tissue. Large changes in intracavernosal pressure occur only after the stiffened tunica albuginea begins to resist tissue expansion.

Folded tissue and crimped collagen fibers permit the flaccid tunica albuginea to change shape during erection, as in other inflating tissues (Fung, 1981, 1984; Canfield and Dobrin, 1987; Orton and Brodie, 1987; Brainerd, 1994). In all these tissues, the collagen fiber extension will increase the flexural stiffness of the inflated structure, both by increasing the Young's modulus of the tissue and by increasing the second moment of area of the structure as a whole. But once the collagen fibers in the tunica albuginea are fully extended, their arrangement in an axial orthogonal array prevents any further shape change of the corpus cavernosum. This is unlike structures reinforced by crossed-helical arrays of fibers, which can change shape when fully inflated (Clark and Cowey, 1958; Wainwright, 1988). The anatomical design of the tunica albuginea therefore not only allows the corpus cavernosum to expand during erection, but stops corpus cavernosum inflation at a fixed and repeatable size and shape.

This study was carried out with the support of a grant from Sigma Xi (19992). Many thanks go to Tall Timbers Research Station for their assistance in collecting tissue, to Angela

Deaton for preparing illustrations and to Charles Pell (Bio-Design Studio) and Steven Vogel (Duke University) for their input in the design of the penis inflator. The Duke University Morphometrics Laboratory provided imaging equipment for morphological measurements. An earlier version of this paper was reviewed by Stephen A. Wainwright, Kathleen K. Smith and V. Louise Roth, all of whom made many suggestions which have substantially improved it. The paper was reviewed in its current form by John E. A. Bertram, John Hermanson and two anonymous reviewers.

References

Andersson, K. E. and Wagner, G. (1995). Physiology of penile erection. *Physiol. Rev.* **75**, 191–236.

Arvy, L. (1978). Le pénis des Cétacés. *Mammalia* **42**, 491–509.

Ashdown, R. R. (1973). Functional anatomy of the penis in ruminants. *Vet. Ann.* **14**, 22–25.

Ashdown, R. R. (1987). Anatomy of male reproduction. In *Reproduction in Farm Animals* (ed. E. S. E. Hafez), pp. 17–34. Philadelphia: Lea and Febiger.

Bitsch, M., Kromann-Andersen, B., Schou, J. and Shontoft, E. (1990). The elasticity and the tensile strength of tunica albuginea of the corpus cavernosum. *J. Urol.* **143**, 642–645.

Brainerd, E. L. (1994). Pufferfish inflation, functional morphology of postcranial structures in *Diodon holocanthus* (Tetradontoformes). *J. Morph.* **220**, 243–261.

Canfield, T. R. and Dobrin, P. B. (1987). Static elastic properties of blood vessels. In *Handbook of Bioengineering* (ed. R. Skalak and S. Chien), pp. 16.1–16.28. New York: McGraw-Hill Co.

Clark, R. B. and Cowey, J. B. (1958). Factors controlling the change of shape of certain nemertean and turbellarian worms. *J. exp. Biol.* **35**, 731–748.

Creed, K. E., Carati, C. J. and Keogh, E. J. (1991). The physiology of penile erection. In *Oxford Reviews of Reproductive Biology*, vol. 13 (ed. S. R. Milligan), pp. 73–95. Oxford: Oxford University Press.

Denny, M. (1988). *Biology and Mechanics of the Wave-Swept Environment*. Princeton: Princeton University Press.

Deysach, L. J. (1939). The comparative morphology of the erectile tissue of the penis with especial emphasis on the probable mechanism of erection. *Am. J. Anat.* **64**, 111–131.

Dodd, J. M. and Dodd, M. H. I. (1985). Evolutionary aspects of reproduction in cyclostomes and cartilaginous fishes. In *Evolutionary Biology of Primitive Fishes*, vol. 103 (ed. R. E. Foreman, A. Gorbman, J. M. Dodd and R. Olsson), pp. 295–319. New York: Plenum Press.

Dowling, H. G. and Savage, J. M. (1960). A guide to the snake hemipenis: a survey of basic structure and systematic characteristics. *Zoologica* **45**, 17–27.

Eberhard, W. G. (1985). *Sexual Selection and Animal Genitalia*. Cambridge: Harvard University Press.

Fung, Y. C. (1981). *Biomechanics: Mechanical Properties of Living Tissues*. Berlin: Springer-Verlag.

Fung, Y. C. (1984). Structure and stress–strain relationship of soft tissues. *Am. Zool.* **24**, 13–22.

Goes, P. M., Wespes, E. and Schulman, C. (1992). Penile extensibility: to what is it related? *J. Urol.* **148**, 1432–1434.

Goldstein, A. M. B., Meehan, J. P., Morrow, J. W., Buckley, P. A. and Rogers, F. A. (1985). The fibrous skeleton of the corpora cavernosa and its probable function in the mechanism of erection. *Br. J. Urol.* **57**, 574–578.

Hanyu, S. (1988). Morphological changes in penile vessels during erection: the mechanism of obstruction of arteries and veins at the tunica albuginea in dog corpora cavernosa. *Urol. Int.* **43**, 219–224.

Hanyu, S., Iwanaga, T., Kano, K. and Sato, S. (1987). Mechanism of penile erection in the dog. *Urol. Int.* **42**, 401–412.

Hsu, G.-L., Brock, G., Martinez-Pineiro, L., Von Heyden, B., Lue, T. F. and Tanagho, E. A. (1994a). Anatomy and strength of the tunica albuginea: its relevance to penile prosthesis extrusion. *J. Urol.* **151**, 1205–1208.

Hsu, G.-L., Brock, G., Von Heyden, B., Nunes, L., Lue, T. F. and Tanagho, E. A. (1994b). The distribution of elastic fibrous elements within the human penis. *Br. J. Urol.* **73**, 566–571.

Hyman, L. H. (1951). *The Invertebrates: Acanthocephala, Aschelminthes and Entoprocta*. New York: McGraw-Hill.

Kelly, D. A. (1997). Axial orthogonal fiber reinforcement in the corpus cavernosum of the nine-banded armadillo (*Dasypus novemcinctus*). *J. Morph.* **233**, 249–255.

Kier, W. M. (1992). Hydrostatic skeletons and muscular hydrostats. In *Biomechanics (Structures and Systems): A Practical Approach* (ed. A. A. Biewener), pp. 205–231. New York: IRL Press.

Kiernan, J. A. (1990). *Histological and Histochemical Methods: Theory and Practice*, 2nd edition. Oxford: Pergamon Press.

King, A. S. (1981). Phallus. In *Form and Function in Birds*, vol. 2 (ed. A. S. King and J. McLelland), pp. 107–147. London: Academic Press.

Koehl, M. A. R., Quillian, K. and Pell, C. (1995). Mechanical consequences of fiber orientation in the walls of hydraulic skeletons. *Am. Zool.* **35**, 53A.

Neville, A. C. (1993). *Biology of Fibrous Composites: Development Beyond the Cell Membrane*. Cambridge: Cambridge University Press.

Nickel, R., Schummer, A., Seiferle, E. and Sack, W. O. (1979). *The Viscera of the Domestic Mammals*, 2nd edition. New York: Springer-Verlag.

Orton, L. S. and Brodie, P. F. (1987). Engulfing mechanics of fin whales. *Can. J. Zool.* **65**, 2898–2907.

Purohit, R. C. and Beckett, S. D. (1976). Penile pressures and muscle activity associated with erection and ejaculation in the dog. *Am. J. Physiol.* **231**, 1343–1348.

Ribeiero, M. G. and Noguiera, J. C. (1990). The penis morphology of the four-eyed opossum *Philander opossum. Anat. Anz.* **171**, 65–72.

Shadwick, R. (1992). Soft composites. In *Biomechanics: Materials: A Practical Approach* (ed. J. F. V. Vincent), pp. 133–164. Oxford: IRL Press.

Smith, J. O. and Sidebottom, O. M. (1969). *Elementary Mechanics of Deformable Bodies*. London: Collier-Macmillan Ltd.

Spencer, A. J. M. (1972). *Deformations of Fibre-Reinforced Materials*. Oxford: Clarendon Press.

Tejada, I. S., Moroukian, P., Tessier, J., Kim, J. J., Goldstein, I. and Frohrib, D. (1991). Trabecular smooth muscle modulates the capacitor function of the penis. *Am. J. Physiol.* **260**, H1590–H1595.

Timoshenko, S. (1957). *Strength of Materials*, part II, *Advanced*, third edition. New York: VanNostrand Reinhold Co.

van Tienhoven, A. (1983). *Reproductive Physiology of Vertebrates*. Ithaca: Cornell University Press.

Vardi, Y. and Siroky, M. B. (1990). Hemodynamics of pelvic nerve induced erection in a canine model. I. Pressure and flow. *J. Urol.* **144**, 794–797.

Vincent, J. (1990). *Structural Biomaterials*. Princeton: Princeton University Press.

Wagner, G. (1981). Erection: physiology and endocrinology. In *Impotence, Physiological, Psychological, Surgical Diagnosis and Treatment* (ed. G. Wagner and R. Green), pp. 24–36. New York: Plenum Press.

Wainwright, S. A. (1988). *Axis and Circumference: The Cylindrical Shape of Plants and Animals*. Cambridge: Harvard University Press.

Wainwright, S. A., Biggs, W. D., Currey, J. D. and Gosline, J. M. (1976). *Mechanical Design in Organisms*. Princeton: Princeton University Press.

Wainwright, S. A., Vosburgh, F. and Hebrank, J. H. (1978). Shark skin: Function in locomotion. *Science* **202**, 747–749.

Wake, M. H. (1998). Cartilage in the cloaca: phallodeal spicules in caecillians (Amphibia: Gymnophiona). *J. Morph.* **237**, 177–186.

Walton, A. (1956). Copulation and natural insemination. In *Marshall's Physiology of Reproduction*, vol. 1, part 1 (ed. A. S. Parkes), pp. 130–160. London: Longmans and Green.

Watson, J. W. (1964). Mechanism of erection and ejaculation in the bull and ram. *Nature* **204**, 95–96.

Woodall, P. F. (1995). The penis of elephant shrews (Mammalia: Macroscelididae). *J. Zool., Lond.* **267**, 399–410.

Woolley, P. and Webb, S. J. (1977). The penis of dasyurid marsupials. In *The Biology of Marsupials* (ed. B. Stonehouse and D. Gilmore), pp. 307–323. Baltimore: University Park Press.

Wourms, J. P. (1981). Viviparity: the maternal–fetal relationship in fishes. *Am. Zool.* **21**, 473–515.

Zug, G. R. (1966). The penial morphology and the relationships of cryptodiran turtles. *Occ. Pap. Mus. Zool. Mich.* **617**, 1–24.